frontiers | Frontiers in Energy Research

TYPE Original Research
PUBLISHED 10 August 2023
DOI 10.3389/fenrg.2023.1177595

OPEN ACCESS

EDITED BY
Zhengmao Li,
Nanyang Technological University,
Singapore

REVIEWED BY
Shuai Yao,
Cardiff University, United Kingdom
Xiaodong Zheng,
Southern Methodist University,
United States
Yunqi Wang,
Monash University, Australia

*CORRESPONDENCE
Xiaoyun Li,
1148917200@qq.com

RECEIVED 01 March 2023
ACCEPTED 18 April 2023
PUBLISHED 10 August 2023

CITATION
Xie W and Li X (2023), Low-carbon economic operation of IES based on life cycle method and hydrogen energy utilization.
Front. Energy Res. 11:1177595.
doi: 10.3389/fenrg.2023.1177595

Low-carbon economic operation of IES based on life cycle method and hydrogen energy utilization

Weiqiang Xie and Xiaoyun Li*

School of Electric Power Engineering, Shanghai University of Electric Power, Shanghai, China

The Integrated Energy System (IES) that coordinates multiple energy sources can effectively improve energy utilization and is of great significance to achieving energy conservation and emission reduction goals. In this context, a low-carbon and economic dispatch model for IES is proposed. Firstly, a hydrogen energy-based IES (H2-IES) is constructed to refine the utilization process of hydrogen energy. Secondly, the carbon emissions of different energy chains throughout their life cycle are analyzed using the life cycle assessment method (LCA), and the carbon emissions of the entire energy supply and demand chain are considered. Finally, a staged carbon trading mechanism is adopted to promote energy conservation and emission reduction. Based on this, an IES low-carbon and economic dispatch model is constructed with the optimization goal of minimizing the sum of carbon trading costs, energy procurement costs, and hydrogen sales revenue, while considering network constraints and constraints on key equipment. By analyzing the model under different scenarios, the introduction of life cycle assessment, staged carbon trading, and hydrogen energy utilization is shown to promote low-carbon and economic development of the comprehensive energy system.

KEYWORDS

integrated energy system, hydrogen energy utilization, life cycle assessment, wind power consumption, low carbon economy

1 Introduction

Currently, the use of fossil fuels has led to serious problems of energy depletion and environmental pollution. Wind and photovoltaic power generation, as renewable clean energy sources, can improve the energy structure and reduce carbon emissions (Yang et al., 2017).

Hydrogen energy has the characteristics of high calorific value and low pollution, and can be coupled with electricity and heat in the integrated energy system (IES) to form an integrated energy system with hydrogen energy (H2-IES). This has important implications for improving overall energy utilization and achieving a reduction in carbon emissions (Xu et al., 2019; Lin et al., 2020; Wan et al., 2021).

There are a large number of literatures on integrated energy systems (IES) research both domestically and abroad. WU (Wu et al., 2021) established an optimization and scheduling model for an IES system that takes into account power-to-gas (P2G) devices and combined cooling, heating, and power (CCHP) units, and verified that introducing diversified energy conversion equipment is beneficial to improving wind power consumption and energy utilization efficiency. ZHENG (Zheng et al., 2021) considered the uncertainty of renewable energy generation and energy demand, and proposed a data-driven stochastic cooperative timing model for electric and gas integrated energy systems, and addressed the energy price formation and settlement issues in an uncertain market by proposing expected locational marginal prices, and demonstrated that the flexibility of P2G can help hedge against uncertainty. QIU (Qiu et al., 2022) explored the advantages of a mixed hydrogen-natural gas transportation system in improving energy utilization efficiency and reducing costs. SHI (Shi et al., 2018) coordinated demand-side flexible loads with P2G scheduling, and verified the optimal scheduling of the system under four scenarios. The scheduling models in these references focus on the operation optimization of IES and ignore the current low-carbon development background.

Currently, carbon trading is regarded as an important mechanism to reduce carbon emissions. LU (Lu et al., 2021) proposes a wind power curtailment strategy that takes into account the thermal and electrical characteristics of Combined Heat and Power (CHP) units based on the carbon trading mechanism. CUI (Cui et al., 2021) analyzes the principle of carbon trading mechanism and introduces an electric-thermal integrated energy system to analyze the impact of carbon trading prices on the system's carbon emissions. ZHANG (Zhang et al., 2020) introduces a reward-penalty carbon trading mechanism in the IES planning model, and uses a two-stage robust optimization model to deal with the uncertainty of electric-thermal loads, verifying the low-carbon and economic performance of the model. HUANG (Huang et al., 2023) proposes a double-layer trading framework with regional carbon emission constraints based on the Stackelberg game theory, in which a virtual power plant with zero carbon emissions is the leader that sets flexible carbon emission permit prices, and analyzes the superiority of this trading mechanism in carbon emissions reduction. WANG, CHENG and WANG (Cheng et al., 2020; Wang et al., 2020; Wang et al., 2022) calculate the carbon emission responsibility borne by the demand side based on the theory of carbon emission flow, and verify that the model that takes into account the demand side's carbon emissions responsibility can stimulate the willingness of the constructed system to reduce emissions.

Given the current installed capacity of new energy generation units, increasing the consumption of new energy can reduce carbon emissions, but the problem of wind power curtailment is prominent due to the anti-peak characteristics of wind power (Yang et al., 2013). WU and QIU (Wu et al., 2021; Qiu et al., 2022) has used P2G to improve wind power consumption, however, most existing studies only consider the conversion of electricity to natural gas in P2G modeling. CUI (Cui et al., 2020) points out that the efficiency of producing natural gas from electricity is 55%, while the efficiency of producing hydrogen from electricity can reach up to 70% (Wei et al., 2018), indicating a need for detailed consideration of the electricity-to-gas conversion process. Currently, we mainly study coal-fired units Carbon in CHP units, gas fired boilers, and hydrogen fuel cell vehicles Emissions, rarely analyzing energy production Carbon emissions from transportation and storage.

In the context of the above, this paper comprehensively considers stepped carbon Trading mechanism, hydrogen energy utilization and optimization of integrated energy system The impact of degree. Compared with existing research, the main innovations and contributions of this article are as follows:

1. Aiming at the incomplete life cycle assessment of carbon emissions from hydrogen energy chains, the LCA (Life Cycle Assessment) method was used to analyze carbon emissions generated during the migration and transformation process of hydrogen energy chains in H2-IES.
2. Aiming at the non-linear efficiency problems of hydrogen energy production and utilization equipment under different operating conditions, a refined model was established to comprehensively reflect the impact of specific energy efficiency characteristics of hydrogen energy equipment on the operation of H2-IES.
3. Considering the role of the carbon trading market, a stepped carbon trading model is established to limit the system's carbon emissions, and the impact of carbon trading parameters on the operation of H2-IES is discussed.

2 H2-IES analysis of a carbon trading mechanism with a stepped structure incorporating LCA energy chain analysis

IES meets its internal energy demands through multiple energy sources and supply equipment. This paper introduces hydrogen production equipment (HPE) and hydrogen fuel cells (HFC) to the traditional model, forming an H2-IES. The specific framework is shown in Figure 1.

2.1 Modeling of hydrogen utilization stage

Hydrogen, as a clean and efficient energy source, has great potential for utilization in various fields such as industry, civilian use, and transportation. The utilization stages of hydrogen in H2-IES include hydrogen production by electrolysis and hydrogen-to-heat-to-electricity conversion. HPE converts electrical energy into hydrogen energy, and fuel cells use hydrogen energy for thermal and electrical production.

1) HPE

$$\begin{cases} P_{\mathrm{HPE,H_2}}(t) = \eta_{\mathrm{HPE}}(t) P_{\mathrm{e,HPE}}(t) \\ \eta_{\mathrm{HPE}}(t) = \sum_{x=1}^{n} \varphi_{\mathrm{HPE},x} \left(\frac{P_{\mathrm{e,HPE}}(t)}{P_{\mathrm{e,HPE}}^{max}} \right)^{x} \\ P_{e,HPE}^{min} \le P_{e,HPE}(t) \le P_{e,HPE}^{max} \\ \Delta P_{e,HPE}^{min} \le P_{e,HPE}(t+1) - P_{e,HPE}(t) \le \Delta P_{e,HPE}^{max} \end{cases} \tag{1}$$

where $P_{\mathrm{e,HPE}}(t)$ is the electrical energy input to HPE at time period t; $P_{\mathrm{HPE,H_2}}(t)$ is the hydrogen energy output of HPE at the time period t; $\eta_{\mathrm{HPE}}(t)$ is the hydrogen production efficiency of HPE during period t; $\varphi_{\mathrm{HPE},x}$ represents polynomial coefficients of hydrogen production efficiency function; $P_{e,\mathrm{HPE}}^{max}$ and $P_{e,\mathrm{HPE}}^{min}$ are the upper and lower limits of electric energy input to HPE respectively; $\Delta P_{e,\mathrm{HPE}}^{max}$ and $\Delta P_{e,\mathrm{HPE}}^{min}$ are the upper and lower climbing limits for HPE respectively.

HPE equipment can be used for wind power curtailment. It can be known from LI (Li et al., 2020), the efficiency of hydrogen

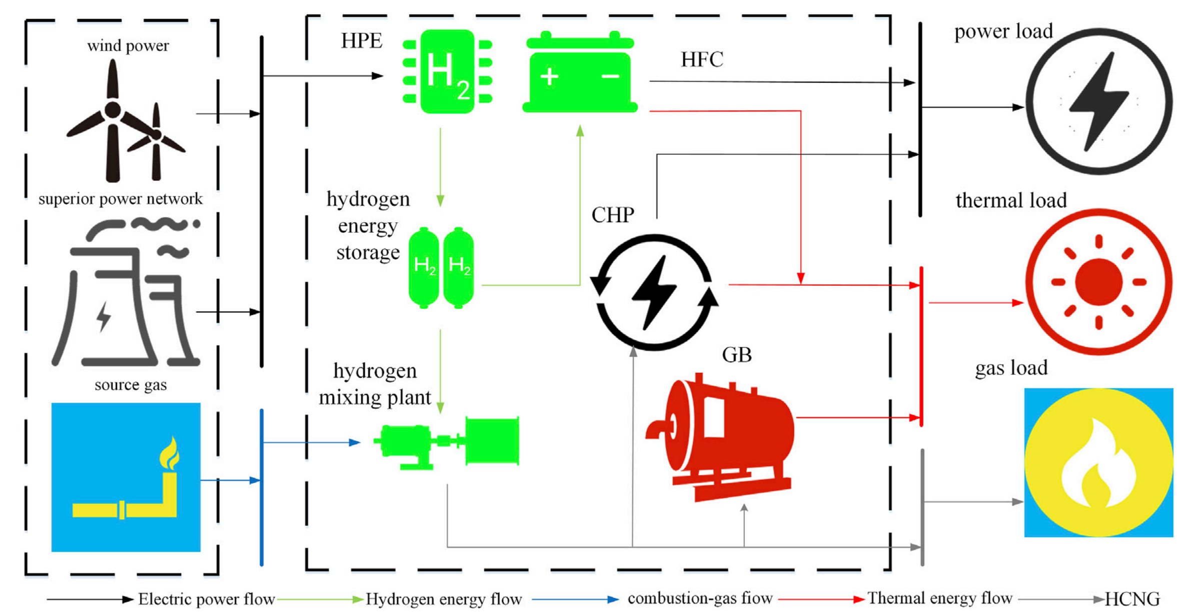

FIGURE 1
Integrated energy system framework.

production equipment is non-linear, and the hydrogen production efficiency gradually decreases as the input power increases to the rated power, while the production output increases. However, the low efficiency leads to an increase in hydrogen production costs. Therefore, considering the economic issues of its output, a flexible operation mode should be adopted. That is, when the hydrogen production revenue exceeds the cost of coal-fired power generation, the coal-fired power should be input to HPE to obtain revenue; otherwise, the coal-fired power will not be input to HPE.

2) HFC

HFC can realize the coupling between hydrogen energy, thermal energy, and electrical energy, strengthen the synergy between different forms of energy in the system, and convert hydrogen energy into electricity and thermal energy through HFC without producing pollutants and carbon dioxide as traditional CHP units do. Therefore, it can promote the clean operation of the system. The HFC model in this paper is as follows:

$$\begin{cases} P_{\mathrm{HFC,e}}(t) = \eta_{\mathrm{HFC,e}}(t) P_{H_2,\mathrm{HFC}}(t) \\ P_{\mathrm{HFC,h}}(t) = \eta_{\mathrm{HFC,h}}(t) P_{H_2,\mathrm{HFC}}(t) \\ \eta_{\mathrm{HFC,e}}(t) = \sum_{x=1}^{n} \varphi_{\mathrm{HFCe},x} \left(\dfrac{P_{H_2,\mathrm{HFC}}(t)}{P_{H_2,\mathrm{HPE}}^{max}} \right)^{x} \\ \eta_{\mathrm{HFC,h}}(t) = \sum_{x=1}^{n} \varphi_{\mathrm{HFCh},x} \left(\dfrac{P_{H_2,\mathrm{HFC}}(t)}{P_{H_2,\mathrm{HPE}}^{max}} \right)^{x} \\ P_{H_2,\mathrm{HFC}}^{\min} \le P_{H_2,\mathrm{HFC}}(t) \le P_{H_2,\mathrm{HFC}}^{\max} \\ \Delta P_{H_2,\mathrm{HFC}}^{\min} \le P_{H_2,\mathrm{HFC}}(t) - P_{H_2,\mathrm{HFC}}(t-1) \le \Delta P_{H_2,\mathrm{HFC}}^{\max} \end{cases} \tag{2}$$

where $P_{H_2,\mathrm{HFC}}(t)$ is the hydrogen energy consumed by HFC at the time period t; $P_{\mathrm{HFC,e}}(t)$ and $P_{\mathrm{HFC,h}}(t)$ are the generating power and heat generation power of HFC in time period t; respectively; $\eta_{\mathrm{HFC,e}}(t)$ and $\eta_{\mathrm{HFC,h}}(t)$ are the conversion efficiency of HFC into electricity and heat energy in t period, respectively; $\varphi_{\mathrm{HFCe},x}$ and $\varphi_{\mathrm{HFCh},x}$ represent the polynomial coefficients of the power generation and heat generation efficiency functions respectively; $P_{H_2,\mathrm{HFC}}^{\max}$and $P_{H_2,\mathrm{HFC}}^{\min}$ are the upper and lower limits of HFC capacity respectively; $\Delta P_{H_2,\mathrm{HFC}}^{\min}$ and $\Delta P_{H_2,\mathrm{HFC}}^{\max}$ are the upper and lower limits of HFC.

In the formula: is the hydrogen energy consumed by HFC in time period t; and are the power generation and heat production power of HFC in time period t, respectively; and are the efficiency of HFC converting hydrogen energy into electrical and thermal energy in time period t; and are the polynomial coefficients of the power generation and heat production efficiency functions, respectively; and are the upper and lower limits of HFC capacity, respectively; is the ramp-up and ramp-down limit of HFC.

2.2 LCA energy chain analysis in IES

2.2.1 LCA energy chain analysis

Life Cycle Assessment (LCA) energy chain analysis consists of three implementation steps: classification, characterization, and quantification (Wang et al., 2019). During the energy production and transmission process in the H2-IES supply process, carbon emissions are generated. If only the carbon emissions during device usage are considered, the overall carbon emissions of the H2-IES cannot be fully reflected. Therefore, the total carbon emissions of each energy chain are calculated using LCA energy chain analysis, which includes the entire process from energy extraction to consumption, taking into account the accompanying effects of material conversion.

2.2.2 Carbon emission analysis of IES based on LCA

WANG (Wang et al., 2019) and HUANG (Huang et al., 2022) respectively analyzed the LCA energy chains of coal-fired power, new energy, natural gas, and energy storage, but did not quantify the carbon emissions of the hydrogen energy chain. The carbon emissions of the hydrogen energy LCA energy chain can be divided into two stages: production (raw material mining and processing) and transportation (raw material transportation and hydrogen transportation). The specific measurement process is as follows:

$$\begin{cases} E_{\mathrm{pH_2}} = QU_pU_{ep}(1+\lambda+\gamma) \\ E_{\mathrm{tH_2}} = \sum_i^I\sum_j^J U_i^j GHG_i^j r_i^j QM_i \end{cases} \tag{3}$$

where $E_{\mathrm{pH_2}}$ and $E_{\mathrm{tH_2}}$ are carbon emission coefficients of production link and transport link respectively; Q is the conversion coefficient of unit standard electricity quantity and energy consumption; U_p is the unit energy consumption of the production process; U_{ep} is the carbon emission factor of production. λ is the unit loss rate in the process of raw material mining; γ is the unit loss in the processing process; I and J represent the sets of transportation methods and fuels, respectively; U_i^j is the energy consumption of the *ith* type of transportation using the *jth* type of fuel; GHG_i^j is the emission equivalent of CO_2 produced by *ith* type of transportation using the *jth* fuel; r_i^j is the proportion of the transportation distance using the *jth* type of fuel for the *ith* type of transportation to the total transportation distance; M_i is the average transportation distance of the *ith* type of transportation.

2.3 Carbon trading model

Carbon trading is essentially establishing reasonable carbon emissions quotas and allowing market-based trading of carbon emissions quotas, thus controlling the trading mechanism of carbon emissions.

2.3.1 Carbon emissions quota model

For major carbon emission sources such as coal-fired power plants, CHP units, and gas boilers, the baseline method is used to determine their carbon emissions quotas (Qu et al., 2018); the carbon emissions quotas for renewable energy units can refer to YANG (Yang et al., 2015). Since the government has not yet set carbon quotas for energy storage devices, the carbon emissions quota for energy storage is set to 0 in this paper.

2.3.2 Actual carbon emission model

The LCA energy chain of H2-IES involves various energy production, transportation, and utilization stages. The carbon emission coefficients of the three stages are quantified using the following formula:

$$E_e = E_{p,e} + E_{t,e} + E_{g,e} \tag{4}$$

Where E_e is the total carbon emissions coefficient of equipment e, g/kWh; $E_{p,e}$ is the total carbon emissions coefficient of the production stage for the corresponding energy type of equipment e; $E_{t,e}$ is the total carbon emissions coefficient of the transportation stage for the corresponding energy type of equipment e; $E_{g,e}$ is the total carbon emissions coefficient of the usage stage for the corresponding energy type of equipment e. Since carbon emissions are related to the operating output of the equipment, the total carbon emissions can be calculated as follows:

$$E_{all} = \sum_{e\in\Omega} E_eP_e \tag{5}$$

where Ω is the set of energy supply and storage equipment; P_e is the power of energy type e; E_{all} is the actual carbon emissions.

Once the actual carbon emissions are obtained, the carbon emissions trading volume involved in the carbon trading market can be calculated.

$$E_{IES} = E_{all} - M_{all} \tag{6}$$

where M_{all} represents the carbon emission quota of the system.

2.3.3 Staggered carbon trading model

The traditional carbon trading mechanism assumes a fixed carbon trading cost throughout the entire scheduling period. If the carbon emissions do not exceed the quota, the excess quota can be traded for profit. Otherwise, the excess carbon emissions must be offset by purchasing additional carbon quotas, which can be expressed as Eq. 7:

$$F_1 = \varpi E_{IES} \tag{7}$$

where F_1 is the carbon trading cost and ϖ represents the unit price of carbon trading.

The cost of tiered carbon trading mechanism is determined by dividing the carbon emission quota into different intervals, with different carbon trading prices for each interval.

$$F_1 = \begin{cases} \varpi E_{IES}, 0 \le E_{IES} < l \\ \varpi(1+\chi)(E_{IES}-l) + \varpi l, l \le E_{IES} < 2l \\ \varpi(1+2\chi)(E_{IES}-2l) + \varpi(2+\chi)l, 2l \le E_{IES} < 3l \end{cases} \tag{8}$$

where l is the length of carbon emission interval; χ is the price growth rate.

3 Consideration of the staircase carbon trading mechanism and the low-carbon economic dispatch model of H2-IES objective function

3.1 Objective function

The optimization objective of the low-carbon economic dispatch model of H2-IES is the sum of carbon trading cost F_1, energy cost F_2 and hydrogen sales revenue F_3:

$$min\,F = min(F_1 + F_2 - F_3) \tag{9}$$

$$F_2 = \sum_{t=1}^T \left[p_{gas}(t)\frac{P_{gas}(t)}{\rho} + f_{grid} \right] \tag{10}$$

$$f_{grid} = \sum_{t=1}^T Cbuy(t)\,max\{P_{grid}(t), 0\} + Csell(t)\,max\{-P_{grid}(t), 0\} \tag{11}$$

$$P_{sale,H_2}(t) = P_{\mathrm{HPE,H_2}}(t) - P_{H_2,\mathrm{HFC}}(t) \tag{12}$$

$$F_3 = \frac{\sum_{t=1}^{T} P_{sale,H_2}(t)}{\nu} p_{H_2}(t) \tag{13}$$

where F is the system operating cost, and f_{grid} is the cost of purchasing and selling electricity; $P_{gas}(t)$ represents the output power of natural gas source at time t; ρ is the heating value of natural gas, which is taken as 9.98 (kWh)/m^3; $p_{gas}(t)$ is the price of natural gas at time t; $Cbuy(t)$; $Csell(t)$ are respectively the system electricity purchasing price and electricity selling price at time t; $P_{grid}(t)$ is the power purchased and sold at time t; if it is greater than 0, it is electricity purchasing, if it is less than 0, it is electricity selling; $P_{sale,H_2}(t)$ is the hydrogen energy sold at time t; ν is the calorific value of hydrogen, taking 4.1 (kWh)/m^3; $p_{H_2}(t)$ is the selling price of hydrogen at time t.

3.2 Constraint condition

3.2.1 Equipment constraints

1) Constraints of HPE and HFC are shown in Eqs 1, 2.
2) Gas Boiler (GB)

$$\begin{cases} P_{\mathrm{GB,h}}(t) = \eta_{\mathrm{GB}} P_{\mathrm{g,GB}}(t) \\ P_{g,GB}^{min} \le P_{\mathrm{g,GB}}(t) \le P_{g,GB}^{max} \\ \Delta P_{g,GB}^{min} \le P_{\mathrm{g,GB}}(t) - P_{\mathrm{g,GB}}(t-1) \le \Delta P_{g,GB}^{max} \end{cases} \tag{14}$$

where $P_{\mathrm{g,GB}}(t)$ is the natural gas power consumption of GB during the time period t; η_{GB} is the conversion efficiency of GB; $P_{\mathrm{g,GB}}^{max}$ and $P_{\mathrm{g,GB}}^{min}$ are the upper and lower limits of GB capacity respectively; $\Delta P_{\mathrm{g,GB}}^{min}$ and $\Delta P_{\mathrm{g,GB}}^{max}$ are the upper and lower limits of GB climbing slope respectively.

3) CHP

$$\begin{cases} P_{\mathrm{CHP,e}}(t) = \eta_{\mathrm{CHP,e}} P_{\mathrm{g,CHP}}(t) \\ P_{\mathrm{CHP,h}}(t) = \eta_{\mathrm{CHP,h}} P_{\mathrm{g,CHP}}(t) \\ P_{g,CHP}^{min} \le P_{g,CHP}(t) \le P_{g,CHP}^{max} \\ \Delta P_{g,CHP}^{min} \le P_{g,CHP}(t) - P_{g,CHP}(t-1) \le \Delta P_{g,CHP}^{max} \end{cases} \tag{15}$$

where $P_{\mathrm{g,CHP}}(t)$ is the natural gas power consumed by CHP during the time period t; $P_{\mathrm{CHP,e}}(t)$ and $P_{\mathrm{CHP,h}}(t)$ are the generating power and heat generating power of CHP in t period; $\eta_{\mathrm{CHP,e}}$ and $\eta_{\mathrm{CHP,h}}$ are the efficiency of conversion of CHP into electricity and heat energy, respectively; $P_{\mathrm{g,CHP}}^{max}$ and $P_{\mathrm{g,CHP}}^{min}$ are the upper and lower limits of CHP capacity respectively; $\Delta P_{\mathrm{g,CHP}}^{max}$ and $\Delta P_{\mathrm{g,CHP}}^{min}$ are the upper and lower limits of CHP climbing slope respectively.

4) Constraints on energy storage operation

According to JIANG (Jiang and Ai, 2019), the models of energy storage devices such as electric and thermal are similar, so this paper adopts a unified modeling approach for electric and thermal energy storage devices.

$$\begin{cases} 0 \le P_{\mathrm{ES},n,\mathrm{cha}}(t) \le B_{\mathrm{ES},n,\mathrm{cha}}(t) P_{\mathrm{ES},n}^{max} \\ 0 \le P_{\mathrm{ES},n,\mathrm{dis}}(t) \le B_{\mathrm{ES},n,\mathrm{dis}}(t) P_{\mathrm{ES},n}^{max} \\ P_{\mathrm{ES},n}(t) = P_{\mathrm{ES},n,\mathrm{cha}}(t)\eta_{\mathrm{ES},n,\mathrm{cha}} - \dfrac{P_{\mathrm{ES},n,\mathrm{dis}}(t)}{\eta_{\mathrm{ES},n,\mathrm{dis}}} \\ S_{n,t} = S_{n,t-1} + P_{\mathrm{ES},n}(t) \\ B_{\mathrm{ES},n,\mathrm{cha}}(t) + B_{\mathrm{ES},n,\mathrm{dis}}(t) = 1 \\ S_n^{min} \le S_{n,t} \le S_n^{max} \end{cases} \tag{16}$$

Where $P_{\mathrm{ES},n,\mathrm{cha}}(t)$ and $P_{\mathrm{ES},n,\mathrm{dis}}(t)$ are the charging and discharging power of the nth energy storage device in time period t; $P_{\mathrm{ES},n}^{max}$ is the maximum power of single charge and discharge of the nth energy storage device; $B_{\mathrm{ES},n,\mathrm{cha}}(t)$ and $B_{\mathrm{ES},n,\mathrm{dis}}(t)$ are binary variables, which are charging and discharging state parameters of the nth energy storage device during t period, respectively; $B_{\mathrm{ES},n,\mathrm{cha}}(t) = 1$ and $B_{\mathrm{ES},n,\mathrm{dis}}(t) = 0$ means in the energized state, whereas said in can put condition; $P_{\mathrm{ES},n}(t)$ is a kind of energy storage device t time the final output power; $\eta_{\mathrm{ES},n,\mathrm{cha}}$ and $\eta_{\mathrm{ES},n,\mathrm{dis}}$ respectively the charge and discharge efficiency of energy storage device; $S_{n,t}$ is the capacity of the nth energy storage device; S_n^{max} and S_n^{min} are respectively the upper and lower limits of the capacity of the nth energy storage device.

3.2.2 Electrical, gas, and heat network constraints

1) Active power balance constraint

$$\begin{aligned} &P_{grid}(t) + P_{wind}(t) + P_{\mathrm{CHP,e}}(t) + P_{\mathrm{HFC,e}}(t) + P_{\mathrm{ES,e,dis}}(t) \\ &\quad = P_{LE}(t) + P_{\mathrm{e,HPE}}(t) + P_{\mathrm{ES,e,cha}}(t) \end{aligned} \tag{17}$$

Where $P_{wind}(t)$ is the wind power output in hour t; $P_{LE}(t)$ is equivalent load at hour t; $P_{\mathrm{ES,e,cha}}(t)$ and $P_{\mathrm{ES,e,dis}}(t)$ is charging and discharging power of electric storage at period t.

2) Thermal power balance constraints

$$\begin{aligned} &P_{\mathrm{HFC,h}}(t) + P_{\mathrm{CHP,h}}(t) + P_{\mathrm{GB,h}}(t) + P_{\mathrm{ES,h,dis}}(t) \\ &\quad = P_{\mathrm{h\_load}}(t) + P_{\mathrm{ES,h,cha}}(t) \end{aligned} \tag{18}$$

Where $P_{\mathrm{h\_load}}(t)$ represents the heat load during period t; $P_{\mathrm{ES,h,cha}}(t)$ and $P_{\mathrm{ES,h,dis}}(t)$ represent the charging and discharging power of the thermal energy storage during period t.

Natural gas equilibrium constraint

$$P_{gas}(t) = P_{g\_load}(t) + P_{\mathrm{g,CHP}}(t) + P_{\mathrm{g,GB}}(t) \tag{19}$$

where $P_{g\_load}(t)$ is the gas load at time period t.

3.3 Model linearization processing

The hydrogen production equipment and fuel cell models constructed in this paper are nonlinear models that require piecewise linearization before being solved using CPLEX.

Step 1: Divide the definition field of the original function independent variable into Q intervals according to the required accuracy. The interval determination method is as follows. When performing piecewise linearization fitting, the linearization function $\tilde{h}_i$ and the nonlinear function h on the ith piecewise linearization interval $D_i = [r_i, r_{i+1}]$ have high estimates and undervalues of errors. The overestimated value refers to the error caused by the high value of $\tilde{h}_i$, while the underestimated value of error refers to the error caused by the low value of $\tilde{h}_i$. Define the maximum error overestimation value $e_{i,h}$, the maximum error underestimation value $e_{i,l}$, and the maximum error value $e_{i,\max}$ as

$$\begin{cases} e_{i,h} = \max\left\{\tilde{h}_i(r_q) - h(r_q) : r_q \in [r_i, r_{i+1}]\right\} \\ e_{i,l} = \max\left\{h(r_q) - \tilde{h}_i(r_q) : r_q \in [r_i, r_{i+1}]\right\} \\ e_{i,max} = \max\{e_{i,h}, e_{i,l}\} \end{cases} \tag{20}$$

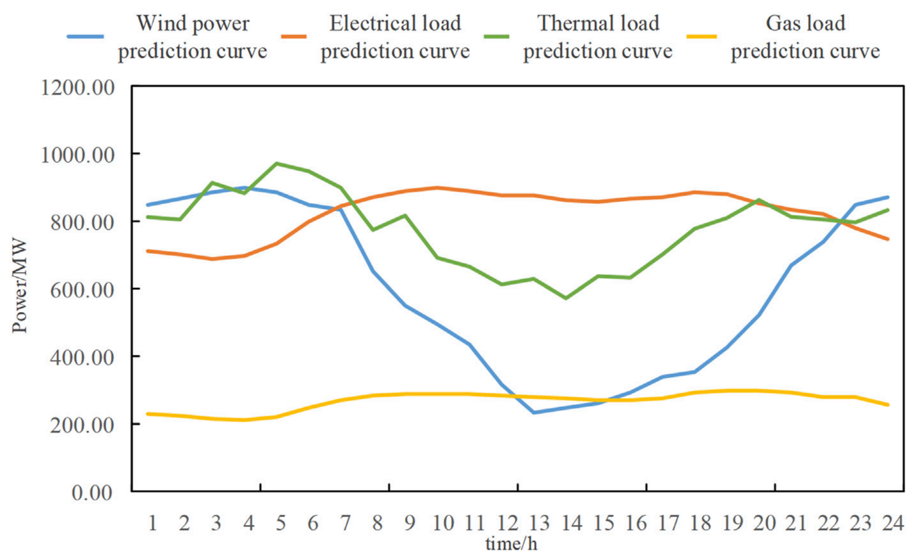

FIGURE 2
Influence of different carbon trading base price on system carbon emission.

TABLE 1 Table of carbon emission from different energy chains.

Energy chain type	Production	Transmission	Use	Carbon emission coefficient/(g/kWh)
natural gas	√	√	√	564.7
wind energy	√	√	—	43
coal power	√	√	√	1380
stored energy	√	√	—	91.33
hydrogen energy	√	√	—	38.9

The calculation idea can be summarized as follows: First, give the maximum error value $e_{\max}$ caused by piecewise linearization, solve hi on D_i, calculate $e_{i,h}$ and $e_{i,l}$ respectively, find the point where the error within the interval is obtained as $e_{i,\max}$. If $e_{i,\max}$ is greater than the predetermined $e_{\max}$, determine a new piecewise linearization interval based on this point and recalculate the error on the new piecewise interval. If it is less than or equal to $e_{\max}$, the calculation ends. Finally, the information of Q piecewise linearized intervals D_i is obtained through iterative calculation. The specific implementation process of this method is shown in Supplementary Appendix B.

Step 2: Add $Q+1$ continuous auxiliary variables $[w_1, w_2, ..., w_{Q+1}]$ and Q *0–1* auxiliary variables $[z_1, z_2, ..., z_Q]$, and satisfy the following equation.

$$\begin{cases} w_1 + w_2 + ... + w_{Q+1} = 1 \\ z_1 + z_2 + ... + z_Q = 1 \\ w_1 \quad 0, w_2 \quad 0, ..., w_{Q+1} \quad 0 \\ w_1 \quad z_1, w_2 \quad z_1 + z_2, ..., w_Q \quad z_{Q-1} \quad z_Q, w_{Q+1} \quad z_Q \end{cases} \tag{21}$$

Step 3: Assume that the determined segment interval is $[r_1, r_2]$, $[r_2, r_3]$, $[r_Q, r_{Q+1}]$,Therefore, the non-linear function $P_{HPE,H_2}(t) = \sum_{x=1}^{n} \varphi_{HPE,x} \frac{P_{e,HPE}(t)^{x+1}}{P_{e,HPE}^{\max}{}^{x}}$ can be replaced by the following linear expression.

$$\begin{cases} P_{e,HPE}(t) = \sum_{q=1}^{Q+1} w_q r_q \\ P_{HPE,H_2}(t) = \sum_{q=1}^{Q+1} w_q P_{HPE,H_2}(r_q) \end{cases} \tag{22}$$

4 Case study analysis

4.1 Case study parameters

To validate the effectiveness of the proposed scheduling strategy, simulation is conducted based on the following load, energy, and equipment data. The various loads of the IES and wind power output prediction results are shown in Figure 2. The parameters of time-of-use electricity prices, various equipment, and energy storage are

TABLE 2 Carbon quota coefficient per unit power.

Energy type	Quota/(g/kWh)
Coal power	798
CHP	424
Wind power	78
Gas heat	152
Heat accumulation	0

shown in Supplementary Appendix Tables A1–A3. The price of natural gas is 0.35 yuan per cubic meter, and that of hydrogen is 3.6 yuan per cubic meter. Interval length l = 2t, price growth χ = 25%, carbon trading base ϖ = 250 yuan/t. $e_{\max}$ is given in advance as 1% of the maximum capacity of the linearized model device.

This paper performs optimization using CPLEX and sets up four operating scenarios for analysis.

Scenario 1: The operational cost of H2-IES without considering carbon trading costs under the tiered carbon trading mechanism; Scenario 2: H2-IES considers the cost of carbon trading under the traditional carbon trading mechanism; Scenario 3: H2-IES considering carbon trading costs under the tiered carbon trading mechanism (the optimization method proposed in this paper); Scenario 4: The traditional combined heat and power system considering carbon trading costs under the tiered carbon trading mechanism.

The total carbon emission coefficient obtained by the LCA energy chain analysis is shown in Table 1. The introduction of carbon trading mechanism is to study the carbon emissions in economic terms. The selection of the carbon emission quota coefficient per unit of electricity output in this paper refers to the relevant data on carbon emission quota allocation issued by the National Development and Reform Commission, and the specific data is shown in Table 2.

4.2 Analysis of dispatch results in different optimization scenarios

Based on the four scenarios mentioned above, the system operating costs were obtained as shown in Table 3. Among them, scenarios 1, 2, and 3 have the same energy supply structure and equipment, and in scenario 4, traditional P2G devices replace HPE and HFC.

Figures 3–5 show the operation conditions of electric load units and thermal load units in Scenario 1, 2 and 3, and the operation results of electric, thermal and gas loads in Scenario 4 are shown in Figure 6.

1 Comparison and analysis of different carbon trading mechanisms

In Scenario 1, with the goal of optimizing traditional economic operations, the system will purchase as much natural gas as possible to produce electricity and heat through CHP, as the gas price is cheaper than the electricity price during all time periods. Before 06:00, wind power is sufficient and the efficiency of GB in producing heat is higher than that of CHP, so most of the heat load is supplied by GB, while CHP is in a state of heat-determined electricity. As the electricity load increases and wind power gradually becomes insufficient, CHP needs to supply more electricity, so it gradually reaches full load and produces the maximum electricity and heat power. The period from 23:00 to 24:00 is the same as before 06:00. In order to maximize profits from selling hydrogen, HPE operates at maximum capacity throughout the day, leading to a minimal sum of energy purchase and hydrogen sales revenue. However, a large amount of energy purchases lead to actual carbon emissions far exceeding the carbon emission quota, requiring the purchase of a large amount of carbon emission quotas from the carbon trading market, resulting in the highest total cost.

In Scenario 2, traditional carbon trading is considered in the optimization process. Due to CHP being cleaner than thermal power and GB, CHP is prioritized in providing electricity and heat power, which is why CHP operates at full capacity throughout the day. In addition, unlike Scenario 1, during the peak load period from 07:00 to 22:00, the revenue from selling hydrogen is lower than the cost of carbon trading, so CHP operates near its lower limit, resulting in a decrease in energy purchase cost.

In Scenario 3, due to the tiered carbon trading mechanism, the revenue from selling hydrogen becomes lower than the cost of purchasing carbon emission quotas from the carbon trading market more quickly, resulting in a further reduction in energy purchase.

TABLE 3 Benefit comparison of each scenario.

Scenario	Parameter value			
	Scenario 1	Scenario 2	Scenario 3	Scenario 4
Carbon emission/kg	14161.5	12777.1	12000	12579
Carbon weight cost/yuan	6236.1	3194.3	4875	5236.9
Energy cost/yuan	4241.2	3265.4	2780.5	3581.4
Gas purchase cost/yuan	11231.2	11622.9	11474.6	10353
Hydrogen sales income/yuan	3574.9	2906.9	1625.9	0
Total cost/yuan	18133.6	15175.7	17504.2	19171.3

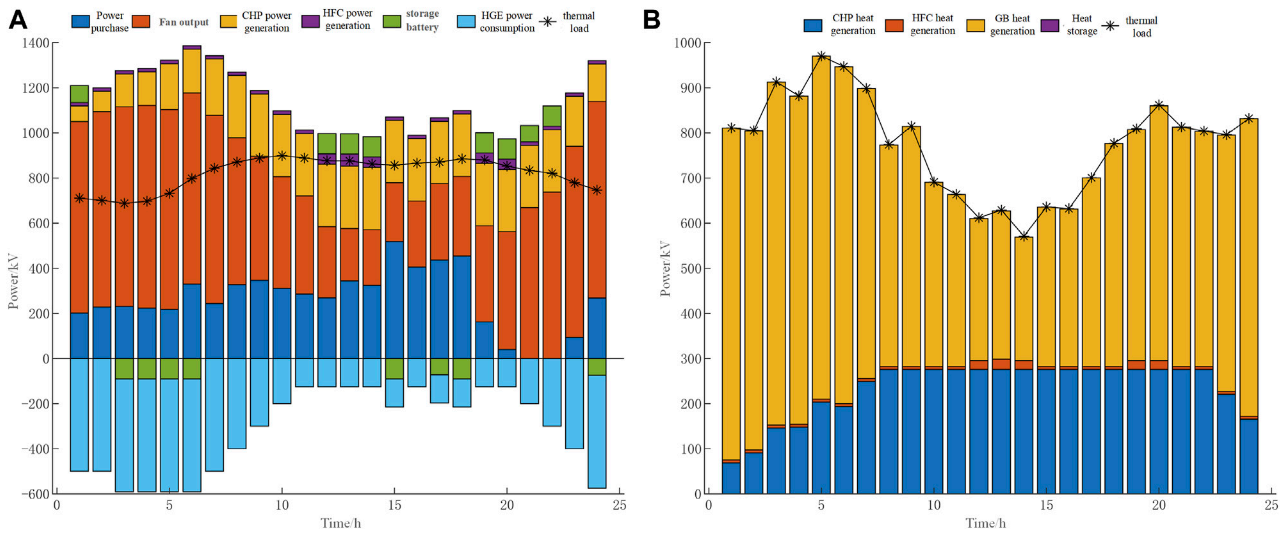

FIGURE 3
Scenario 1 electric **(A)** and thermal **(B)** power blance diagram.

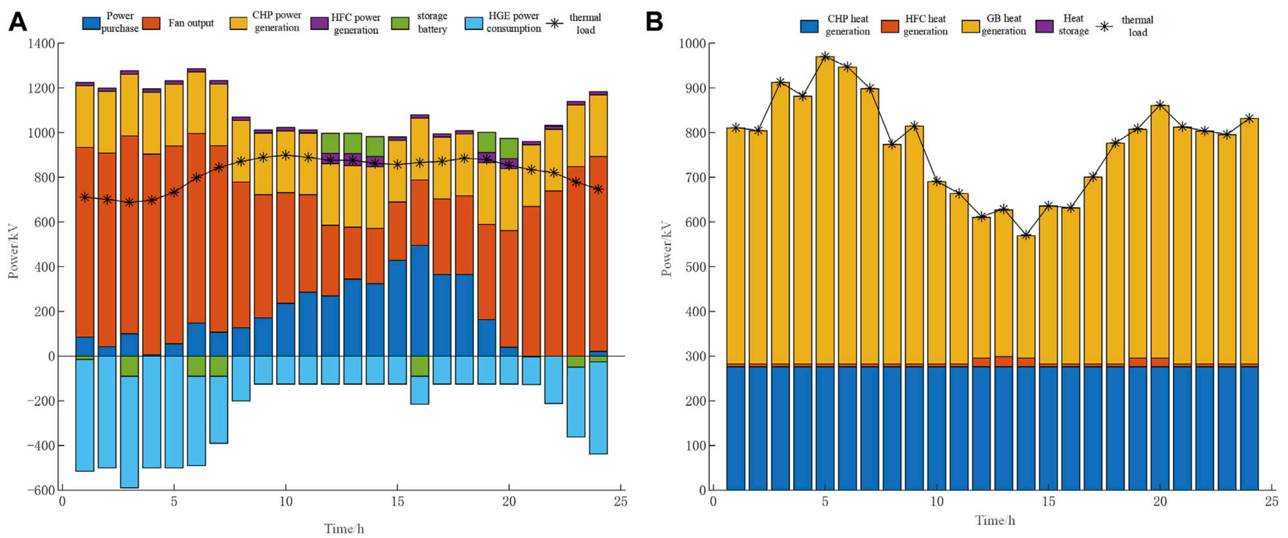

FIGURE 4
Scenario 2 electric **(A)** and thermal **(B)** power blance diagram.

Figure 7 shows a comparison of the total electricity generated by all types of units throughout the day in the three scenarios. According to Figure 7, in the dispatching cycle, the on-grid electricity of coal-fired units in Scenario 1 is the highest, while that in Scenario 3 is the lowest. The difference between Scenario 2 and Scenario 3 lies in the output of HFC equipment. This is because the high carbon trading cost under stepped carbon trading forces HFC to consume hydrogen for energy supply to reduce carbon emissions, which proves that the use of stepped carbon trading is conducive to improving the output of cleaning units. In addition, due to the income from hydrogen sales, surplus wind power in the three scenarios will produce hydrogen through HPE, absorbing all wind power.

2) Comparison Analysis between H2-IES and Traditional CHP Integrated Energy Systems

Scenario 4 includes a P2G system, which can also absorb excess wind power and convert it into natural gas to supply the GB, CHP, or gas load, resulting in the lowest total purchasing cost. However, the P2G conversion efficiency is not high, and the hydrogen undergoes multiple processes of loss after being synthesized into natural gas through a methane reactor before

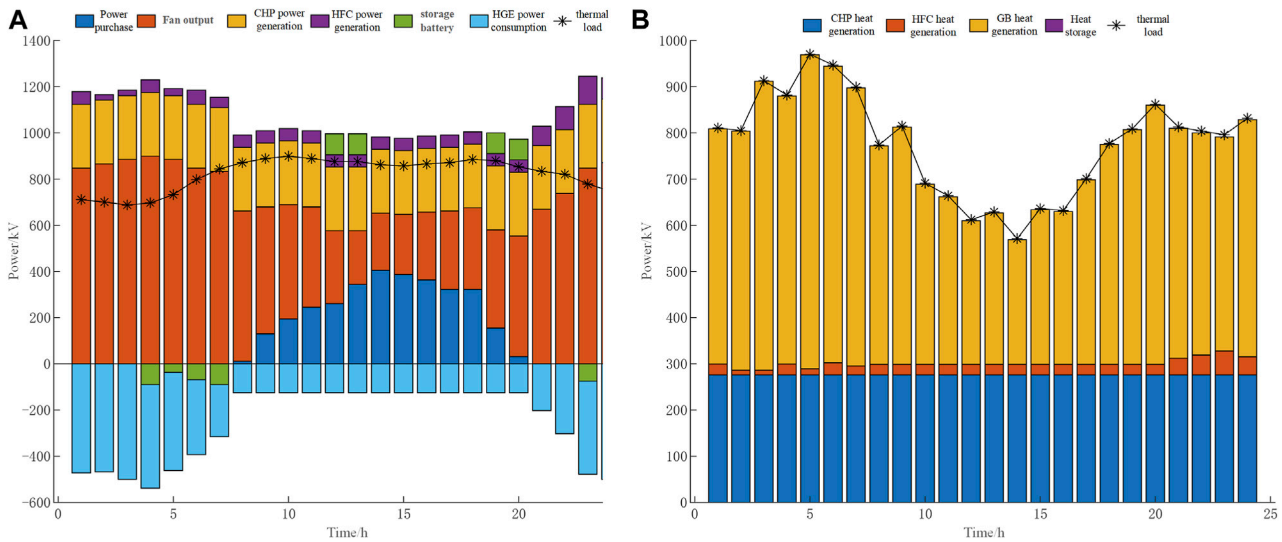

FIGURE 5
Scenario 3 electric **(A)** and thermal **(B)** power blance diagram.

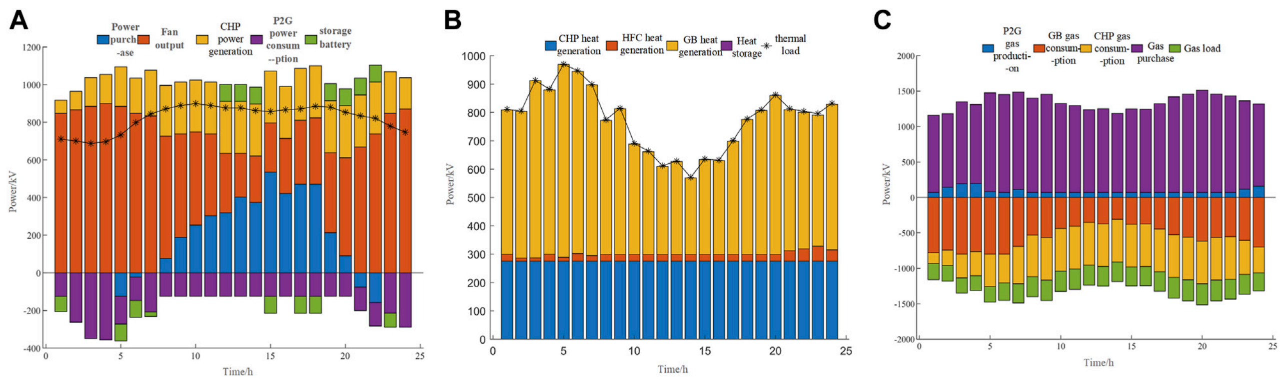

FIGURE 6
Scenario 4 electric **(A)**, thermal **(B)** and gas **(C)** power blance diagram.

being delivered to the GB or CHP. Although P2G can absorb some of the carbon dioxide, burning natural gas will also emit carbon dioxide. In contrast, in the H2-IES system, the HFC uses hydrogen for thermal and electrical production, reducing losses and directly utilizing clean energy, thus reducing carbon emissions. Since all the hydrogen is converted into natural gas in the P2G system, there is a lack of revenue from selling hydrogen, and the economic cost has not decreased.

4.3 Benefit analysis under different carbon trading prices

With the development of society, in order to reduce emission intensity, there is a possibility of changes in the carbon trading base price, price growth rate, and interval length in the stepped carbon trading mechanism. Changes in these parameters will affect the output of various units in the system. Figure 8 shows the impact trend of changes in carbon trading base price on system carbon emissions and total cost in Scenario 3.

According to Figure 8, as the carbon trading base price increases, the weight of carbon trading costs in the total system cost increases, and the carbon trading mechanism imposes stronger restrictions on carbon emissions. Although the carbon emissions of both Scenario 2 and Scenario 3 will decrease as the carbon trading price increases, the decrease in Scenario 3 is faster than that in Scenario 2. When the carbon trading price is less than 45 yuan/t, both Scenario 2 and Scenario 3 provide heat and electricity to the system by increasing the output of relatively clean CHP, thereby reducing carbon

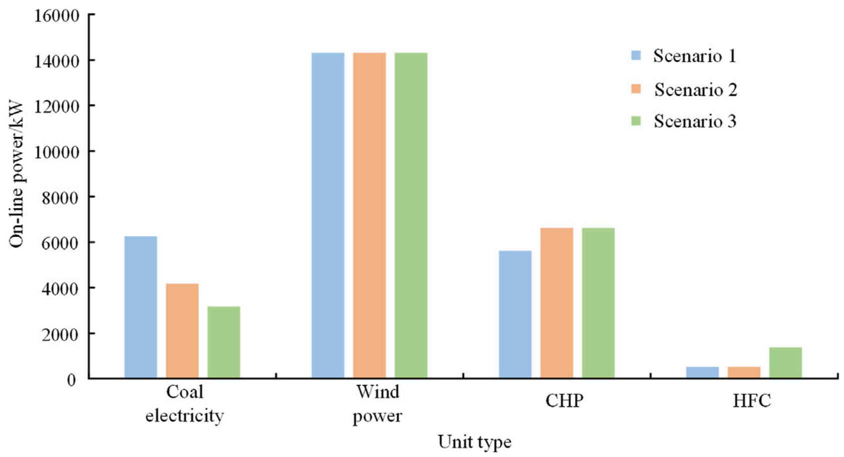

FIGURE 7
The online power of each unit in each scenario.

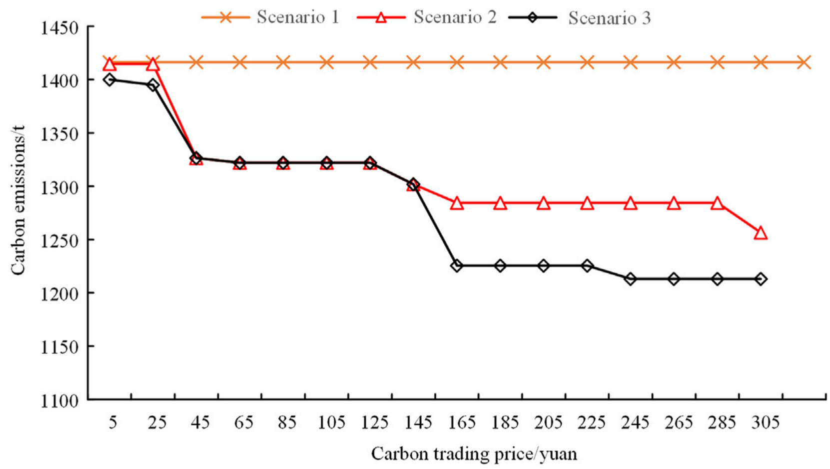

FIGURE 8
Influence of different carbon trading base price on system carbon emission.

emissions. When the carbon trading price is greater than 145 yuan/t, the system reduces its electricity purchases and increases the output of HFC for heat and electricity to reduce carbon emissions. In contrast, Scenario 2 can only affect the purchased electricity when the carbon trading price is greater than 285 yuan/t, indicating that considering the stepped carbon trading is more favorable for the low-carbon operation of the system. In Scenario 3, when the carbon trading base price increases to 245 yuan/t, the output distribution of each equipment in the system tends to be stable, and the carbon emissions also tend to be stable, so the carbon emissions are less affected by changes in the carbon trading base price; due to the increase in carbon trading costs, the total system cost also increases.

According to the above analysis, it can be seen that when the carbon trading base price is greater than a certain value, the system tends to be stable and carbon emissions reach their minimum, indicating that simply raising the base price cannot further reduce emissions, but instead leads to cost increases. Therefore, in Scenario 3, a carbon trading base price of 165 yuan per ton should be selected to balance emissions reduction and economic feasibility.

Based on the analysis between carbon emissions reduction and system costs, high-emission entities face the cost of paying for carbon quotas or fines under carbon trading policies, or buying low-carbon technologies from low-emission entities. If there is no technological innovation, simply increasing the carbon trading price cannot further reduce carbon emissions but instead leads to cost escalation. In contrast, low-emission entities can compensate for their technological innovation and production costs by selling surplus quotas and low-carbon technologies, which will encourage them to increase their

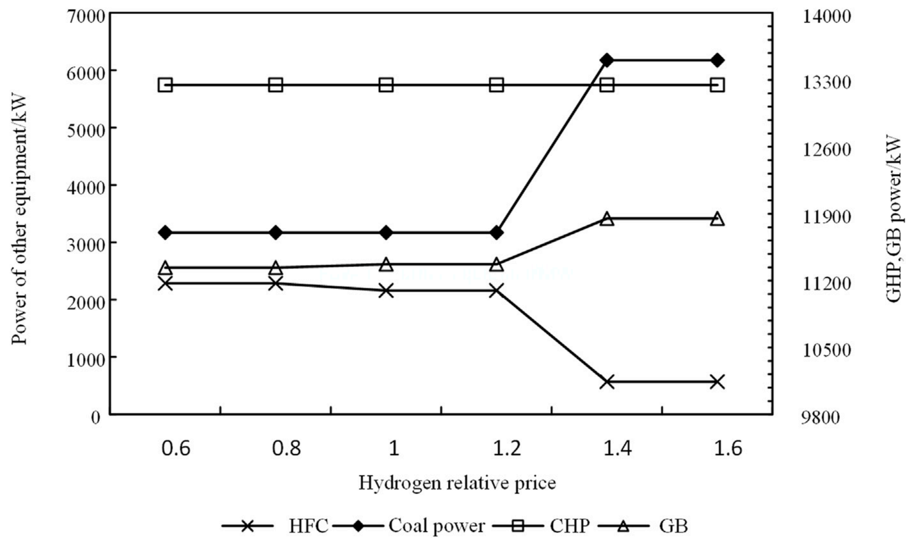

FIGURE 9
Diagram of the hydrogen relative price on system operating cost.

investment in low-carbon technologies and create a virtuous circle. Therefore, under carbon trading policies, carbon emitters can only achieve reduced carbon emissions and reduced costs through technological improvements.

4.4 Impact of relative price fluctuations of hydrogen and natural gas on system economics

When analyzing the impact of relative price fluctuations between hydrogen and natural gas on the system economy, it is assumed that the natural gas price remains constant while the hydrogen price fluctuates up and down by 3.6 yuan/m^3. The resulting relative economic relationship is shown in Figure 9.

According to Figure 9, when the relative price of hydrogen and natural gas fluctuates in a large range (0.6–1.6), it does not affect the output of CHP units. When the relative price is at 1.2, if the price of hydrogen decreases, the output of the HFC equipment increases, because the equipment has no carbon emissions during the entire operation process, which means that the carbon trading cost is higher than the hydrogen sales revenue. If the consumption potential of hydrogen energy in China continues to increase, leading to changes in the supply and demand relationship of hydrogen energy and the price rises, the system will increase the purchase of electricity and reduce the output of HFC to ensure hydrogen sales revenue.

5 Conclusion

This article presents a dispatch model for integrated energy systems (IES) based on the life cycle method and a tiered carbon trading mechanism, taking into account the demands for electricity, heat, and gas loads and the operating characteristics of IES units. Different carbon trading mechanisms and carbon trading benchmark prices were compared and analyzed, and the impact of carbon trading prices on system carbon emissions and the influence of different hydrogen/natural gas prices on system operation were examined. The conclusions drawn are as follows:

1) Taking into account the carbon emissions of each energy chain in IES makes the system's carbon emissions more accurate. Introducing a tiered carbon trading mechanism can adjust the output of each device, and setting a reasonable carbon trading price can guide the system's carbon emissions.
2) The proposed H2-IES low-carbon optimization model can promote wind power consumption while leveraging the high energy efficiency of hydrogen energy. Additionally, it can improve system economics by selling hydrogen gas. When the relative price of hydrogen and natural gas is low, HFC can share part of the energy supply demand of CHP and GB, reducing their carbon emissions and further reducing carbon emissions.

Data availability statement

The original contributions presented in the study are included in the article/Supplementary Material, further inquiries can be directed to the corresponding author.

Author contributions

WX participated in the design of this study, performed the statistical analysis, and drafted the manuscript. XL carried out the study and collected important background information.

Conflict of interest

The authors declare that the research was conducted in the absence of any commercial or financial relationships that could be construed as a potential conflict of interest.

Publisher's note

All claims expressed in this article are solely those of the authors and do not necessarily represent those of their affiliated organizations, or those of the publisher, the editors and the reviewers. Any product that may be evaluated in this article, or claim that may be made by its manufacturer, is not guaranteed or endorsed by the publisher.

Supplementary material

The Supplementary Material for this article can be found online at: https://www.frontiersin.org/articles/10.3389/fenrg.2023.1177595/full#supplementary-material

References

Cheng, Y. H., Zhang, N., Zhang, B. S., Kang, C. Q., Xi, W. M., and Feng, M. S. (2020). Low-carbon operation of multiple energy systems based on energy-carbon integrated prices. *IEEE Trans. smart grid* 11 (2), 1307–1318. doi:10.1109/TSG.2019.2935736

Cui, Y., Yang, S., Zhong, W. Z., Wang, Z., Zhang, P., and Zhao, Y. T. (2020). Optimaal thermoelectric dispatching of regional integrated energy system with power-to-gas. *Power Syst. Technol.* 44 (11), 4254–4264. doi:10.13335/j.1000-3673.pst.2019.2468

Cui, Y., Zeng, P., Zhong, W. Z., Cui, W. L., and Zhao, Y. T. (2021). Low-carbon economic dispatch of electricity-gas-heat integrated energy system based on ladder-type carbon trading. *Electr. Power Autom. Equip.* 41 (03), 10–17. doi:10.16081/j.epae.202011030

Huang, H. X., Li, Z. M., Mohasha Isuru Sampath, L. P., Yang, J. W., and Nguyen, H. D. (2023). Blockchain-enabled carbon and energy trading for network-constrained coal mines with uncertainties. *IEEE Trans. Sustain. Energy* 2023, 1–12. doi:10.1109/TSTE.2023.3240203

Huang, J. g., Xiong, H. j., Li, Z. X., and Wang, T. (2022). Capacity configuration optimization of buileding inttegrated engrgy system considering fine energy storage mode. *Electr. Measurement& Instrum.* 59 (03), 82–91. doi:10.19753/j.issn1001-1390.2022.03.011

Jiang, C. F., and Ai, X. (2019). Integrated energy system operation opitimization model considering uncertainty of multi-energy coupling units. *Power Syst. Technol.* 43 (08), 2843–2854. doi:10.13335/j.1000-3673.pst.2019.0197

Li, X. S., Sui, Q., Lin, X. N., Wang, Z. X., Wu, C. T., Wei, F. R., et al. (2020). A flexible load control strategy for power grid considering fully consumption of surplus wind power and global benefits. *Proceeding CSEE* 40 (18), 5885–5897. doi:10.13334/j.0258-8013.pcsee.191028

Lin, Z. H., Jiang, C. W., Chen, M. H., Shang, H. Y., Zhao, H. W., Yang, Z., et al. (2020). Low-carbon economic operation of integrated energy systenm considering flexible loads. *Electr. Power Constr.* 41 (05), 9–18. doi:10.12204/j.issn.1000-7229.2020.05.002

Lu, H. P., Xie, L. R., and Gao, W. (2021). Cogeneration-storage-electric boiler wind power consumption strategy with carbon trading. *Electr. Measurement& Instrum.* 2021, 1–11. Available at: http://kns.cnki.net.shiep.vpn358.com/kcms/detail/23.1202.TH.20210831.1125.002.html (Accessed: February 13, 2020).

Qiu, B., Mu, H. B., Wang, K., Zhang, Z. C., and Yang, Z. (2022). An optimal scheduling model of hydrogen coupling IES considering the mixed transportation of hydrogen and natural gas. *Proc. CSU-EPSA.* 34 (8), 51–59. doi:10.19635/j.cnki.csu-epsa.000935

Qu, K. P., Huang, L. N., Yu, T., and Zhang, X. S. (2018). Decentralized dispatch of multi-area integrated energy systems with carbon trading. *Proc. CSEE* 38 (03), 697–707. doi:10.13334/j.0258-8013.pcsee.170602

Shi, S. S., Wang, H. J., Fang, C., Ling, Z., Yang, X., and Li, Y. (2018). "Optimal scheduling of integrated energy system combined with demand side flexible loads," in *Proceedings of the international conference on information Technology and electrical engineering* (New York, NY: Assoc Computing Machinery). 10036-9998 USA, 1–6. doi:10.1145/3148453.3306290

Wan, W. X., Ji, Y. N., Yin, L., and Wu, H. (2021). Application and prospect of carbon trading in the planning and operation of integrated energy system. *Electr. Meas. &Instrumentation* 58 (11), 39–48. doi:10.19753/j.issn1001-1390.2021.11.006

Wang, Y. Q., Qiu, J., Tao, Y. C., Zhang, X., and Wang, G. B. (2020). Low-carbon oriented optimal energy dispatch in coupled natural gas and electricity systems. *Appl. energy* 280 (15), 115948. doi:10.1016/j.apenergy.2020.115948

Wang, Z. S., Shi, Y., Tang, Y. M., Men, X. Y., Cao, J., and Wang, H. J. (2019). Low carbon economy operation and energy efficiency analysis of integrated energy systems considering LCA energy chain and carbon trading mechanism. *Proceeding CSEE* 39 (06), 1614–1626+858. doi:10.13334/j.0258-8013.pcsee.180754

WangQiu, Y. Q. J., and Tao, Y. C. (2022). Robust energy systems scheduling considering uncertainties and demand side emission impacts. *Energy* 239, 122317. doi:10.1016/j.energy.2021.122317

Wei, F. R., Sui, Q., Lin, X. N., Li, L., Chen, L., Zhao, B., et al. (2018). Energy control scheduling optimization strategy for coal-wind- hydrogen energy grid under consideration of the efficiency featyres of hydrogen production equipment. *Proceeding CSEE* 38 (05), 1428–1439. doi:10.13334/j.0258-8013.pcsee.170044

Wu, J., de, G., Tan, Z. F., and Zhang, S. (2021). Multi-objective coordinated optimization model for integrated energy systems with power-to-gas and combined-cooling-heating-power technologies. *Electr. Measurement& Instrum.* 58 (05), 20–30. doi:10.19753/j.issn1001-1390.2021.05.004

Xu, H., Dong, S. F., He, Z. X., Shi, Y. S., Wang, L., and Liu, Y. Q. (2019). Electro-thermal comprehensive demand response based on muti-energy complementarity. *Power Syst. Technol.* 43 (02), 480–489. doi:10.13335/j.1000-3673.pst.2018.2234

Yang, D., Liu, J. R., Yang, J. X., and Ding, J. (2015). Carbon footprint of wind turbine by life cycle assessment. *Acta Sci. Cricumstantiae* 35 (03), 927–934. doi:10.13671/j.hjkxxb.2014.0906

Yang, J. G., Liu, W. M., Li, S. X., Deng, T. H., Shi, Z. P., and Hu, Z. C. (2017). Optimal operation scheme and Benefit analysis of wind-hydrogen power systems. *Electr. Power Constr.* 38 (01), 106–115. doi:10.3969/j.issn.1000-7229.2017.01.014

Yang, N., Wang, B., Liu, D. C., Zhao, J., and Wang, H. (2013). An integrated supply-demand stochastic optimization method considering large-scale wind power and flexible load. *Proc. CSEE* 33 (16), 63–69+17. doi:10.13334/j.0258-8013.pcsee.2013.16.015

Zhang, X. H., Liu, X. Y., and Zhong, J. Q. (2020). Integrated energy system planning considering a reward and punishment ladder-type carbon trading and electric-thermal transfer load uncertainty. *Proc. CSEE* 40 (19), 6132–6142. doi:10.13334/j.0258-8013.pcsee.191302

Zheng, X. D., Xu, Y., Li, Z. M., and Chen, H. Y. (2021). Co-optimisation and settlement of power-gas coupled system in day-ahead market under multiple uncertainties. *IET Renew. power Gener.* 15 (8), 1632–1647. doi:10.1049/rpg2.12073

Nomenclature

IES	integrated energy system
H2-IES	integrated energy system with hydrogen energy
LCA	life cycle assessment
P2G	power to gas
CCHP	combined cooling, heating and power
CHP	combined heat and power
HPE	hydrogen production equipment
HFC	hydrogen fuel cell
GB	gas boiler
$P_{e,HPE}(t)$	the electrical energy input to HPE at time period t
$P_{HPE,H_2}(t)$	the hydrogen energy output of HPE at the time period t
$\eta_{HPE}(t)$	the hydrogen production efficiency of HPE during period t
$\varphi_{HPE,x}$	the polynomial coefficients of hydrogen production efficiency function
$P_{e,HPE}^{max}$	the upper limit of electric energy input to HPE
$P_{e,HPE}^{min}$	the lower limit of electric energy input to HPE
$\Delta P_{e,HPE}^{max}$	the upper climbing limit for HPE
$\Delta P_{e,HPE}^{min}$	the lower climbing limit for HPE
$P_{H_2,HFC}(t)$	the hydrogen energy consumed by HFC at the time period t
$P_{HFC,e}(t)$	the generated power of the HFC during the t period
$P_{HFC,h}(t)$	the heat generating power of the HFC during the t period
$\eta_{HFC,e}(t)$	the efficiency of converting HFC into electrical energy during the t period
$\eta_{HFC,h}(t)$	the efficiency of converting HFC into heat energy during the t period
$\varphi_{HFCe,x}$	the polynomial coefficient of the power generation efficiency function
$\varphi_{HFCh,x}$	the polynomial coefficient of the heat production efficiency function
$P_{H_2,HFC}^{max}$	he upper limit of HFC capacity
$P_{H_2,HFC}^{min}$	the lower limit of HFC capacity
$\Delta P_{H_2,HFC}^{min}$	the upper climbing limit for HFC
$\Delta P_{H_2,HFC}^{max}$	the lower climbing limit for HFC
E_{pH_2}	the carbon emission coefficient of the production process
E_{tH_2}	the carbon emission coefficient in transportation
Q	the conversion coefficient of unit standard electricity quantity and energy consumption
U_p	the unit energy consumption of the production process
U_{ep}	the carbon emission factor of production
λ	the unit loss rate in the process of raw material mining
γ	the unit loss in the processing process
I	the set of transportation methods
J	the set of fuel
U_i^j	the energy consumption of the *ith* type of transportation using the *jth* type of fuel

GHG_i^j	the emission equivalent of CO_2 produced by *ith* type of transportation using the *jth* fuel
r_i^j	the proportion of the transportation distance using the *jth* type of fuel for the *ith* type of transportation to the total transportation distance
M_i	the average transportation distance of the *i*th type of transportation
E_e	the total carbon emissions coefficient of equipment *e*, g/kWh
$E_{p,e}$	the total carbon emissions coefficient of the production stage for the corresponding energy type of equipment *e*
$E_{t,e}$	the total carbon emissions coefficient of the transportation stage for the corresponding energy type of equipment *e*
$E_{g,e}$	the total carbon emissions coefficient of the usage stage for the corresponding energy type of equipment *e*
Ω	the set of energy supply and storage equipment
P_e	the power of energy type *e*
E_{all}	the actual carbon emissions
M_{all}	the carbon emission quota of the system
F_1	the carbon trading cost
ϖ	the unit price of carbon trading
l	the length of carbon emission interval
χ	the price growth rate
F	the system operating cost
f_{grid}	the cost of purchasing and selling electricity
$P_{gas}(t)$	the output power of natural gas source at time *t*
ρ	the heating value of natural gas, 9.98(kWh)/m^3
$p_{gas}(t)$	the price of natural gas at time *t*
$p_{gas}(t)$	the system power purchase price at time *t*
$Csell(t)$	the system electricity selling price at time *t*
$P_{grid}(t)$	the power purchased and sold at time *t*; if it is greater than 0, it is electricity purchasing, if it is less than 0, it is electricity selling
$P_{sale,H_2}(t)$	the hydrogen energy sold at time *t*
v	the calorific value of hydrogen, 4.1(kWh)/m^3
$p_{H_2}(t)$	the selling price of hydrogen at time *t*
$P_{g,GB}(t)$	the natural gas power consumption of GB during the time period *t*
η_{GB}	the conversion efficiency of GB
$P_{g,GB}^{max}$	the upper limit of GB capacity
$P_{g,GB}^{min}$	the lower limit of GB capacity
$\Delta P_{g,GB}^{min}$	the upper climbing limit for GB
$\Delta P_{g,GB}^{max}$	the lower climbing limit for GB
$P_{g,CHP}(t)$	the natural gas power consumed by CHP during the time period *t*
$P_{CHP,e}(t)$	the generating power of CHP in *t* period
$P_{CHP,h}(t)$	the heat generating power of CHP in *t* period
$\eta_{CHP,e}$	the efficiency of conversion of CHP into electricity
$\eta_{CHP,h}$	the efficiency of conversion of CHP into heat energy
$P_{g,CHP}^{max}$	the upper limit of CHP capacity
$P_{g,CHP}^{min}$	the lower limit of CHP capacity
$\Delta P_{g,CHP}^{max}$	the upper climbing limit for CHP

$\Delta P_{g,CHP}^{min}$	the lower climbing limit for CHP
$P_{ES,n,cha}(t)$	the charging power of the *nth* energy storage device in time period *t*
$P_{ES,n,dis}(t)$	the discharging power of the *nth* energy storage device in time period *t*
$P_{ES,n}^{max}$	the maximum power of single charge and discharge of the *nth* energy storage device
$B_{ES,n,cha}(t)$	the charging state parameters of the *nth* energy storage device during *t* period
$B_{ES,n,dis}(t)$	the discharging state parameters of the *nth* energy storage device during *t* period
$P_{ES,n}(t)$	a kind of energy storage device *t* time the final output power
$\eta_{ES,n,cha}$	the charge efficiency of energy storage device
$\eta_{ES,n,dis}$	the discharge efficiency of energy storage device
$S_{n,t}$	the capacity of the *nth* energy storage device
S_n^{max}	the upper limit of the capacity of the *nth* energy storage device
S_n^{min}	the lower limit of the capacity of the *nth* energy storage device
$P_{wind}(t)$	the wind power output in hour *t*
$P_{LE}(t)$	the equivalent load at hour *t*
$P_{ES,e,cha}(t)$	the charging power of electric storage at period *t*
$P_{ES,e,dis}(t)$	the discharging power of electric storage at period *t*
$P_{h\_load}(t)$	the heat load at time period *t*
$P_{ES,h,cha}(t)$	the charging power of thermal energy storage at time period *t*
$P_{ES,h,dis}(t)$	the discharging power of thermal energy storage at time period *t*
$P_{g\_load}(t)$	the gas load at time period *t*